



Calculation of The Nuclear Matter Density Distributions and Form Factors For The Ground State of ^{12}Be and ^{14}Be Nuclei

R. A. Radhi, A. K. Hamoudi and W. Z. Majeed*

Department of Physics, College of Science, University of Baghdad, Baghdad, Iraq.

Abstract

The ground state charge, neutron and matter densities for two-neutron halo nuclei ^{12}Be and ^{14}Be are calculated within a two-frequency shell model approach. In the description of the halo nuclei it is important to take into account a model space for ^{10}Be and ^{12}Be different from the two halo neutrons which have to be treated separately in order to explain their properties. The structures of the halo ^{12}Be and ^{14}Be nuclei show that the dominant configurations when the two halo neutrons distributed over the $1d$ shell orbits. Elastic Coulomb scattering form factors of these two exotic nuclei are also studied through the combination of the density distributions of the ^{10}Be , ^{12}Be core and the two halo neutrons. The effects of the neutron halos on the electron scattering form factors are explored. The form factors for the two exotic ^{12}Be and ^{14}Be nuclei are compared with those of the stable ^9Be nuclei. It is found that the difference in the calculated charge form factors between halo and stable nuclei is attributed mainly to the difference in the center of mass correction which depends on the mass number and the size parameter (b).

PACS number(s): 25.30.Bf; 21.60.Cs; 21.10.Gv; 27.20+n.

Keywords: Neutron-rich exotic nuclei; Shell model calculations; nucleon density distributions of halo nuclei; elastic electron scattering form factors.

حساب توزيعات كثافة المادة النووية وعوامل التشكل للحالة الارضية للنواتين بريليوم 12 و بريليوم 14

رعد عبد الكريم راضي، عادل خلف حمودي و وسن زهير مجيد

قسم الفيزياء، كلية العلوم، جامعة بغداد، بغداد، العراق.

الخلاصة:

تم حساب توزيعات الكثافة البروتونية و النيوترونية والمادة النووية للنوى الهالة الغنية بالنيوترونات ^{12}Be و ^{14}Be باستخدام نموذج القشرة النووي ذو الترددتين. لدراسة النوى الهالة من المهم الاخذ بنظر الاعتبار استخدام فضاء لنيوكليونات القلب ^{10}Be و ^{12}Be مختلف عما هو لنيوكليونات الهالة. من خلال النتائج وجد ان التركيب المهيمن للنواتين ^{14}Be , ^{12}Be هو عند وجود نيوكليونات الهالة في المدار $1d$. كذلك تم دراسة تأثير وجود نيوترونين خارج القلب على عوامل التشكل الكولومية المرنة من خلال ربط توزيعات الكثافة للقلب ^{10}Be و ^{12}Be مع نيوترونين الهالة. عوامل التشكل للنواتين الغريبتين ^{12}Be و ^{14}Be قورنت مع عوامل التشكل

*Email: wasan_zmz@yahoo.com

للنواة المستقرة ${}^9\text{Be}$. وجد ان الاختلاف بين النوى الهالة ونظيرتها المستقرة يعود الى التباين في عامل تصحيح مركز الكتلة والذي يعتمد على العدد الكتلي وثابت المتذبذب التوافقي (b).

1. Introduction

The study of the properties of extremely neutron or proton rich nuclei of light elements is considered as an important and exciting research topic in modern nuclear physics. The term "halo" refers to the weakly bound nucleon or nucleons forming a cloud of low density around a core of normal density. It appeared first in a paper by Hansen and Jonson in 1987 [1]. Since then it has become the label for a few light exotic nuclei with weakly bound nucleons in spatially extended states where the radius of the halo system is significantly larger than the normal nuclear radius.

Since the first observation of ${}^{14}\text{Be}$ and ${}^{17}\text{B}$ in 1973 [2] and ${}^{12}\text{Be}$ in 1965 [3], interest in these nuclei has greatly increased. Some properties, such as the mass and matter radius have been studied and reported by Liatard et al. [4], Tanihata et al.[5] and Ozawa et al. [6]. These anomalously large matter radii have interpreted as being an indication of a neutron halo, which is a feature seen specifically in very neutron-rich and loosely bound nuclei, such as ${}^{11}\text{Li}$ and ${}^{11}\text{Be}$.

Based on Talmi and Unna's description of ${}^{11}\text{Be}$ as a ${}^{10}\text{Be}$ core plus a $1s_{1/2}$ neutron [7], Barker predicted that low lying 0^+ states in ${}^{12}\text{Be}$ should be formed with the same ${}^{10}\text{Be}$ core and a pair of neutrons in the $1s_{1/2}$, $1p_{1/2}$, or $1d_{1/2}$ orbit. Theoretical calculations which study the mixing with intruder orbitals from the sd shell also exist. Clustering structure [8,9,10] or few-body structure with a ${}^{12}\text{Be}$ composed from a ${}^{10}\text{Be}$ core plus two valence neutrons[11,12] have been investigated as well.

The halo structure of ${}^{14}\text{Be}$ has been confirmed by Zahar et al. [13] in a fragmentation experiments of ${}^{14}\text{Be}$ on a ${}^{12}\text{C}$ target. They suggest a strong correlation between the two external neutrons.

The ${}^{14}\text{Be}$ nucleus has been investigated in the three cluster generated coordinate method, involving several ${}^{12}\text{Be}+n+n$ configurations by Descouvemout [14]. The ${}^{12}\text{Be}$ core nucleus was described in the harmonic oscillator model with all possible configurations in the p-shell. A strong enhancement of the root mean square (rms) radius with respect to the ${}^{12}\text{Be}$ core was

obtained, in agreement with experiment. The microscopic wave functions were used to investigate several aspects of the ${}^{14}\text{Be}$ spectroscopy. In addition to the rms radius, he also calculate proton and neutron densities, both in ${}^{14}\text{Be}$ and in the ${}^{12}\text{Be}$ core. These quantities provide more complete information than the rms radius.

Ilieva [15] investigated the nuclear matter density distributions of the exotic ${}^{12}\text{Be}$, ${}^{14}\text{Be}$ and ${}^8\text{B}$ nuclei by elastic proton scattering in inverse kinematics. The experimental results on the isotopes ${}^{12}\text{Be}$ and ${}^{14}\text{Be}$ presented together with their theoretical interpretation in the frame of the Glauber multiple scattering theory. A comparison with several theoretical microscopic calculations were also made. Some preliminary results for nucleus ${}^8\text{Be}$ and their interpretation were displayed as well.

The current experimental technique for recognizing neutron halo and proton halo are mostly based on the measurement of reaction cross sections of the nucleus-nucleus collision and of the momentum distributions of nucleus breakup. There are complex processes where the strong and electromagnetic interactions among nucleons play a role. Despite the fact that this type of experiments has achieved most important success for halo phenomena, it is motivating to look for a new probe to refine the study of neutron halo in neutron rich-nuclei. Electron-nucleus scattering has confirmed to be tremendous tool for the study of nuclear structure, particularly for the study of electromagnetic properties of nuclei. It has given much consistent information on proton density distributions of stable nuclei. The electron-nucleus scattering is a better technique for the accurate study of the long tail behavior in the nucleon density distribution of the exotic neutron-rich nuclei.

In the present work, the two neutron halo structure of ${}^{12}\text{Be}$ and ${}^{14}\text{Be}$ are studied assuming that the two valence neutrons forming the halo. Shell- model configuration mixing is carried out by using a model space for the core nucleus different from that of the two halo neutrons. This assumption is supported by the fact that the

valence neutrons are distributed in a spatial region which is much larger than the core.

The obtained density distributions are used to calculate the electron scattering form factors and compared with stable charge form factors to explore the effects of the neutron halo on the charge distributions and electron scattering form factors.

2. Theory

The form factors for electron scattering between nuclear states J_i and J_f involving angular momentum transfer J are expressed as [16],

$$F_{J,t_z}(q) = \sqrt{\frac{4\pi}{2J_i+1}} \frac{1}{N_{t_z}} \left\langle J_f \left\| \sum_{i=1}^{N_{t_z}} \hat{T}_{J,t_z}(q,i) \right\| J_i \right\rangle \quad (1)$$

where the normalization factor N_{J,t_z} is defined as

$$N_{t_z} = \begin{cases} Z \text{ for } t_z = 1/2 \text{ (protons)} \\ N \text{ for } t_z = -1/2 \text{ (neutrons)} \end{cases} \quad (2)$$

and q is the momentum transfer. The longitudinal (Coulomb) multipole operator \hat{T}_{J,t_z} is given by

$$\hat{T}_{J,t_z}(q,i) = \int d^3r j_J(qr) Y_{JM}(\Omega) \hat{\rho}_{t_z}(\vec{r},i) \quad (3)$$

where $j_J(qr)$ is the spherical Bessel's function and $\hat{\rho}_{t_z}(\vec{r},i)$ is the protons/neutrons density operator which is given by

$$\hat{\rho}_{t_z}(\vec{r},i) = \delta(\vec{r} - \vec{r}_i) \quad (4)$$

Equation (3) reduced to

$$\hat{T}_{J,t_z}(q,i) = j_J(qr_i) Y_{JM}(\Omega_i) \quad (5)$$

The reduced matrix element in equation (1) can be written as a sum over elements of the one-body density matrix (OBDM) elements and the corresponding reduced single-particle matrix element [17]

$$\left\langle J_f \left\| \sum_{i=1}^{N_{t_z}} \hat{T}_{J,t_z} \right\| J_i \right\rangle = \sum_{a,b} \text{OBDM}(J_i, J_f, a, b, J, t_z) \langle a \left\| \hat{T}_{J,t_z} \right\| b \rangle \quad (6)$$

where a and b label the single particle states ($a \equiv n_a \ell_a j_a$ and $b \equiv n_b \ell_b j_b$). The OBDM is defined as [17]

$$\text{OBDM}(J_i, J_f, a, b, J, t_z) = \frac{\langle J_f \left\| [a_{a,t_z}^+ \otimes \tilde{a}_{b,t_z}]^{(J)} \right\| J_i \rangle}{\sqrt{2J+1}} \quad (7)$$

The reduced single-particle matrix elements of the Coulomb operator in equation (6) become:

$$\langle a \left\| \hat{T}_{J,t_z} \right\| b \rangle = \int_0^\infty dr r^2 j_J(qr) \langle j_a \left\| Y_J \right\| j_b \rangle R_{n_a \ell_a}(r) R_{n_b \ell_b}(r) \quad (8)$$

where $R_{n\ell}(r)$ is the harmonic oscillator radial wave function.

The Coulomb form factor given in equation (1) becomes:

$$F_{J,t_z}(q) = \frac{1}{N_{t_z}} \sqrt{\frac{4\pi}{2J_i+1}} \sum_{a,b} \text{OBDM}(J_i, J_f, a, b, J, t_z) \langle j_a \left\| Y_J \right\| j_b \rangle \int_0^\infty dr r^2 R_{n_a \ell_a}(r) R_{n_b \ell_b}(r) j_J(qr) \quad (9)$$

and can be written as

$$F_{J,t_z}(q) = \frac{4\pi}{N_{t_z}} \int_0^\infty dr r^2 j_J(qr) \rho_{J,t_z}(r) \quad (10)$$

where $\rho_{J,t_z}(r)$ is nucleon density distribution and is given by

$$\rho_{J,t_z}(r) = \frac{1}{\sqrt{4\pi}} \frac{1}{\sqrt{2J_i+1}} \quad (11)$$

$$\sum_{a,b} \text{OBDM}(J_i, J_f, a, b, J, t_z) \langle j_a \left\| Y_J \right\| j_b \rangle R_{n_a \ell_a}(r) R_{n_b \ell_b}(r)$$

As the model space wave functions have good isospin, it is appropriate to evaluate the OBDM elements by means of isospin-reduced matrix elements. The relation between the triply reduced OBDM and the proton or neutron OBDM is [18],

$$\begin{aligned} \text{OBDM}(t_z) &= (-1)^{T_f - T_z} \sqrt{2} \begin{pmatrix} T_f & 0 & T_i \\ -T_z & 0 & T_z \end{pmatrix} * \\ &\text{OBDM}(T=0)/2 \\ &+ 2t_z (-1)^{T_f - T_z} \sqrt{6} \begin{pmatrix} T_f & 1 & T_i \\ -T_z & 0 & T_z \end{pmatrix} * \\ &\text{OBDM}(T=1)/2 \end{aligned} \tag{12}$$

where the triply reduced OBDM(T) elements are given by

$$\text{OBDM}(J_i, J_f, \alpha, \beta, J, T) = \frac{\langle \Gamma_f \parallel [a_\alpha^\dagger \otimes \tilde{a}_\beta]^{J,T} \parallel \Gamma_i \rangle}{\sqrt{2J+1} \sqrt{2T+1}} \tag{13}$$

Here, Greek symbols are utilized to indicate quantum numbers in coordinate space and isospace

$$\alpha \equiv at_a, \beta \equiv bt_b, \Gamma_i = J_i T_i \text{ and } \Gamma_f = J_f T_f$$

The OBDM elements contain all the information about transitions of given multi polarities which are embedded in the model space wave functions. Shell model calculations are performed using the code OXBASH [19] with specified model space and effective interaction to generate the OBDM elements.

For the ground state $J=0$, and $J_i = J_f$ and $\ell_a = \ell_b, j_a = j_b$.

The ground state density distribution takes the form,

$$\rho_{t_z}(r) = \frac{1}{4\pi} \frac{1}{\sqrt{2J_i+1}} \sum_{a,b} \text{OBDM}(J_i, J_i, a, b, J=0, t_z) \sqrt{2j_a+1} R_{n_d a}(r) R_{n_d a}(r) \tag{14}$$

The normalization condition of the above ground state density is:

$$4\pi \int_0^\infty dr r^2 \rho_{t_z}(r) = N_{t_z} \tag{15}$$

and the elastic $J=0$ form factor at $q=0$, is equal to one.

Inclusion of the finite nucleon size correction $F_{fs}(q)$ and the center of mass correction $F_{cm}(q)$ in the calculations requires multiplying

the form factor of Eq. (10) by these corrections. The nucleon finite size form factor is [20],

$$F_{fs}(q) = [1 + (q/4.33 \text{ fm}^{-1})^2]^{-2} \tag{16}$$

and the center of mass correction is:

$$F_{cm}(q) = e^{q^2 b^2 / 4A} \tag{17}$$

where A is the nuclear mass number and b is the harmonic-oscillator size parameter, for halo nuclei b equal to the average of b_{core} and b_{halo} . Introducing these corrections into Eq. (10),

$$F_{J,t_z}(q) = \frac{4\pi}{N_{t_z}} \int_0^\infty dr r^2 \rho_{J,t_z}(r) j_J(qr) F_{fs}(q) F_{cm}(q) \tag{18}$$

As the halo nuclei are oversized and easily broken system consisting of a compact core plus a number of outer nucleons loosely bound and specially extended far from the core, it is suitable to separate the ground state density distribution of equation (14) into two parts, one is connected with the core nucleons and the other one with the hole nucleons, so the matter density distribution for the whole halo nucleus becomes:

$$\rho_m(r) = \rho_{p+n}^{\text{core}}(r) + \rho_{p(n)}^{\text{halo}}(r) \tag{19}$$

The corresponding rms radii are given by

$$\langle r^2 \rangle_g^{1/2} = \frac{4\pi}{g} \int_0^\infty dr r^4 \rho_g(r) \tag{20}$$

where g represents the corresponding number of nucleons in each case.

The corresponding elastic scattering $J=0$ form factor (C0) is written in the following form,

$$F_{0,g}(q) = \frac{4\pi}{g} \int_0^\infty dr r^2 j_0(qr) \rho_g(r) \tag{21}$$

The average occupation number in each orbit (n_{a,t_z}) is given by

$$n_{a,t_z} = \sqrt{\frac{2j_a+1}{2J_i+1}} \text{OBDM}(J_i, J_i, a, a, 0, t_z) \tag{22}$$

The total longitudinal form factor is given by

$$|F(q)|^2 = \sum_j |F_j|^2 \quad (23)$$

3. Results and Discussion

Charge, neutron and matter densities of the ^{12}Be ($S_{2n} = 3.67$ MeV, $\tau_{1/2} = 20$ ms) [21,22] and ^{14}Be ($S_{2n} = 1.34$ MeV, $\tau_{1/2} = 4.35$ ms) [23] exotic two-neutron halo nuclei are calculated using different model spaces for the core and the extra two halo neutrons. The calculations based on using two-frequency shell model [24,25], with size parameters for the core different from those for the two halo neutrons in order to reproduce the measured charge and matter rms. Also electron scattering form factors are calculated for these nuclei using Plane Wave Born Approximation (PWBA).

Shell model calculations were performed with shell model code OXBASH [19], where the one-body density matrix (OBDM) elements in spin-isospin formalism are obtained. The densities taken from Ref. [15] for Gaussian-Halo (G-H) parameterization used in the present calculations as a fitted density of ^{12}Be and for Gaussian-Gaussian (G-G) parameterization as a fitted density of ^{14}Be nuclei. The neutron drip line ^{12}Be ($J^\pi T = 0^+2$) and ^{14}Be ($J^\pi T = 0^+3$), which coupled a ^{10}Be core ($J^\pi T = 0^+1$) and outer two neutrons ($J^\pi T = 0^+1$) forming the ^{12}Be nucleus halo and a ^{12}Be core ($J^\pi T = 0^+2$) plus two neutrons system ($J^\pi T = 0^+1$) forming the ^{14}Be nucleus halo. The different model spaces are chosen for the core and the extra two neutrons. The configurations $(1s_{1/2})^4$, $(1p)^6$ and $(1s_{1/2})^4$, $(1p)^8$ are used for ^{10}Be and ^{12}Be , respectively.

A value of $b_{\text{core}} = 1.5$ fm is chosen for ^{10}Be , which gives the rms matter radius equal to 2.173 fm, which is consistent with measured value 2.18 ± 0.02 [15]. A value of $b_{\text{core}} = 1.797$ fm is chosen for ^{12}Be , which gives the rms matter radius equal to 2.645 fm, which is consistent with the measured value $2.59(6)$ fm [26]. Three different configurations are considered for the description of the two halo neutrons in ^{12}Be and ^{14}Be . These two neutrons are assumed to be in a pure $1d_{3/2}$, or a pure $1d_{5/2}$, a pure $2s_{1/2}$ and mixing of the sd orbits. In the sd model space all orbits in $2s-1d$ shells are considered, where the universal shell

model (USD)[27] is used for the sd -shell orbits. To reproduce the matter radii of ^{12}Be (2.82 ± 0.12 fm [15]) and ^{14}Be ($3.16(38)$ fm [26]), a value of $b_{\text{halo}} = 2.45$ fm is used in the case of ^{12}Be and $b_{\text{halo}} = 3.45$ fm for ^{14}Be . These values of b_{halo} give the matter radius of ^{12}Be equal to 2.72 fm and for ^{14}Be equal to 3.456 fm which agree with the measured values.

The matter density distributions $\rho_m(r)$ are displayed in Figure 1 and Figure 2 for ^{12}Be and for ^{14}Be , respectively. The solid curve is the calculated matter density obtained with the assumption that the outer two neutrons move in the sd model space. The dashed curve and dash-dotted curve are the calculated matter density when the outer two neutrons move in pure d orbits and a pure s orbit, respectively. The filled circles are the fitted matter densities taken from Ref. [15]. It is evident from this figure that the calculated matter density distribution represented by the solid curve is in an excellent accordance with that of the dashed curve, and they coincide with each other throughout the whole range of r . These calculations agree well with the fitted data better than the other configurations. The average occupation numbers of the two neutrons using the sd model space for ^{12}Be and ^{14}Be are

$$n_{1d} = 1.6992, \quad n_{2s_{1/2}} = 0.3008$$

The $1d$ shell is the dominant configuration for the two-neutron halo. Hence, the result of the $1d$ shell configuration almost coincides with those of the sd mixed configurations. A long tail is exhibited in the calculated matter density distribution which is consistent with the fitted one.

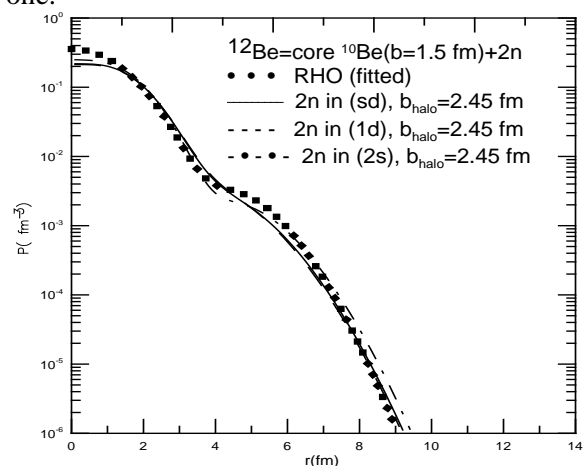


Figure 1- Matter density distributions of ^{12}Be .

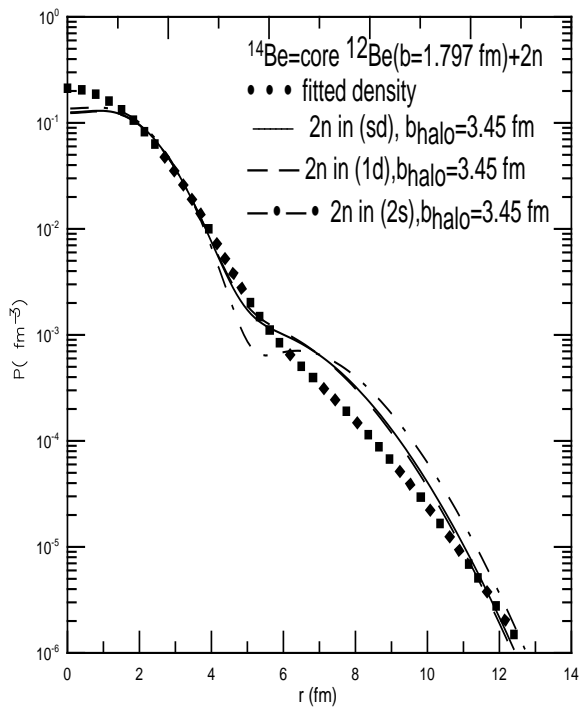


Figure 2-Matter density distributions of ¹⁴Be.

Figure 3 and Figure 4 show the core (protons + neutrons) (dashed curve) and the two halo neutrons (dash- dotted curve) contributions to the matter density of ¹²Be and ¹⁴Be, respectively. The long tail is due to the outer halo neutrons.

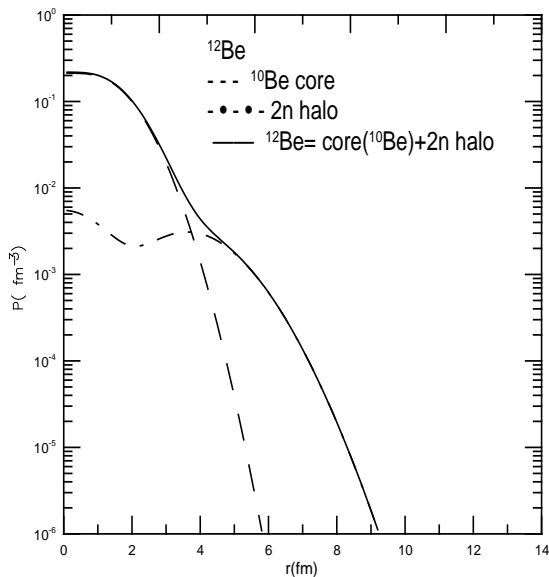


Figure 3- Density distributions of ¹²Be.

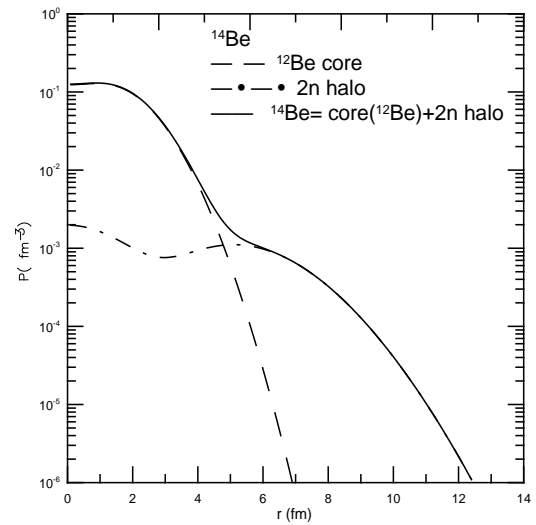


Figure 4-Density distributions of ¹⁴Be.

Figure 5 and Figure 6 show the calculated proton and neutron density displayed as dashed and dash-dotted curves, respectively. The long tail behavior is noticeably seen in the distribution of the neutron density. This behavior is related to the existence of the outer two neutrons in the halo orbits. The difference between the neutron and proton rms radii is $R_n - R_p = 2.984 - 2.121 = 0.863$ fm, and $R_n - R_p = 3.957 - 2.541 = 1.416$ fm for ¹²Be and ¹⁴Be, respectively which provides an additional evidence for the halo structure of these nuclei.

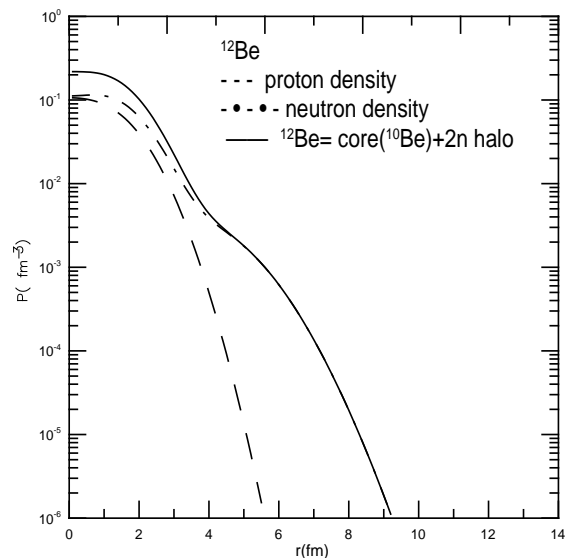


Figure 5-Neutron, proton and matter density distributions of ¹²Be.

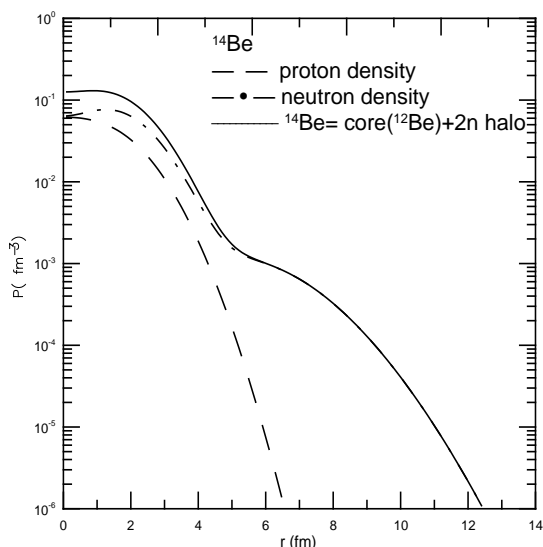


Figure 6- Neutron, proton and matter density distributions of ^{14}Be .

As shown above, ^{12}Be is adopted as the core of the halo nucleus ^{14}Be . The comparison between the core size of ^{14}Be ($R_c = 1.797$ fm) and the matter radius of ^{12}Be ($R_m = 2.72$ fm), indicate that the free ^{12}Be and the core have different behavior as shown in Figure 7. When free, ^{12}Be exhibits an extended structure. In this mass region breaking of the $N=8$ neutron shell closure is observed due to intruder orbitals from the next sd shell. This leads to an extended matter distribution due to neutrons on the $s_{1/2}$ orbital. While, when ^{12}Be is within the ^{14}Be nucleus most probable its last neutrons occupy the p shell which is the available one, as in Figure 7.

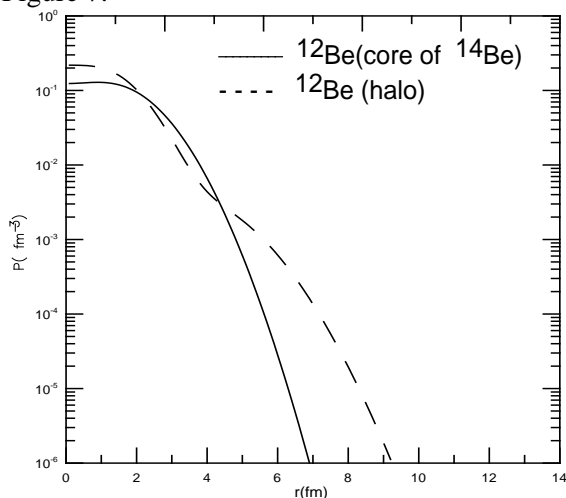


Figure 7- Comparison between the matter density distributions of ^{12}Be and the core density of ^{14}Be .

For the sake of completeness of the comparison, the reference ^9Be stable nuclei is chosen, where experimental data (electron scattering form factors) are available [20]. A size parameter for the harmonic oscillator radial wave functions is chosen to be $b=1.68$ fm for ^9Be , to reproduce the measured rms matter radius ($2.38(1)\text{fm}$ [26]).

To see the effects of the addition of neutrons to form halo nuclei on the form factors, the calculated charge ($C0+C2$) form factors of ^9Be compared with the measured data taken from Ref. [20] are presented. These results are displayed in Figure 8, using effective charges equal to $1.35e$ and $0.35e$, for the protons and neutrons, respectively, for $C2$ to account the core polarization effects [17]. The experimental data are very well reproduced. $C0$ and $C2$ contributions are shown in this figure by the dotted and dashed curves, respectively.

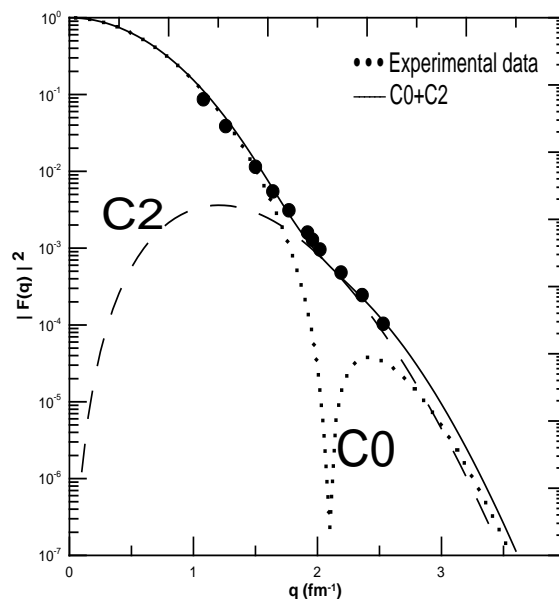


Figure 8- Elastic charge form factors of ^9Be .

Figure 9 and Figure 10, show the charge longitudinal $C0$ elastic electron scattering form factors for ^{12}Be and ^{14}Be halo nucleus respectively, calculated with PWBA, displayed as dashed curve in comparison with that of ^9Be (solid curve). The significant difference between the form factors of the exotic neutron-drip line $^{12,14}\text{Be}$ and that of stable ^9Be is the difference in the center of mass correction which depends on the mass number and the size parameter b which is assumed in this case equal to the average of b_{core} and b_{halo} .

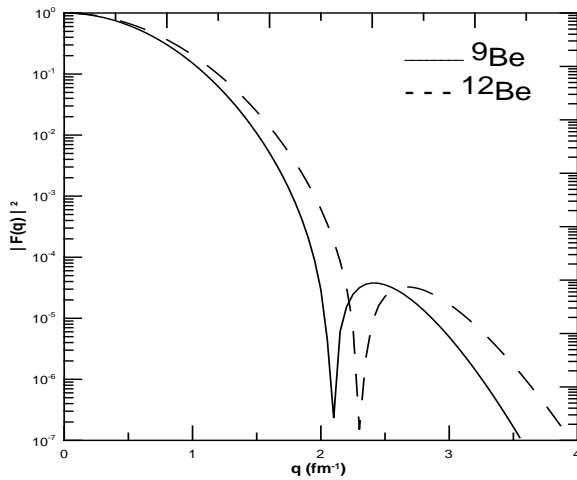


Figure 9-Elastic matter form factors of ${}^9,{}^{12}\text{Be}$.

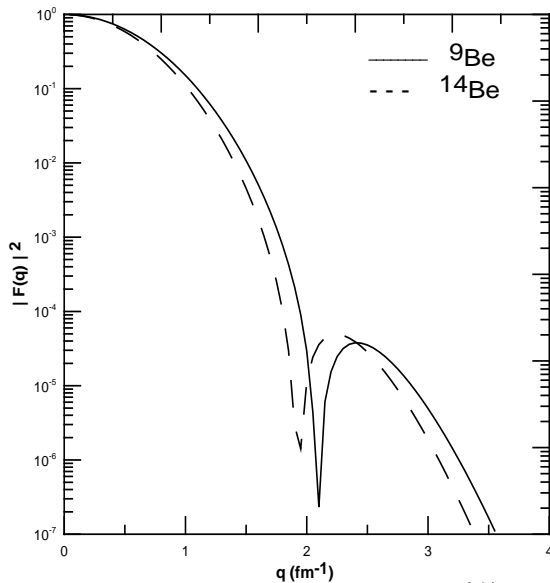


Figure 10-Elastic matter form factors of ${}^9,{}^{14}\text{Be}$.

4. Conclusions

The ground state proton, neutron and matter density distributions of unstable neutron-rich ${}^{12}\text{Be}$ and ${}^{14}\text{Be}$ exotic nuclei are investigated using the two-frequency shell model approach. Elastic electron scattering from these two exotic nuclei are also investigated. The long tail behavior, considered as a distinctive feature of halo nuclei, is evidently revealed in the calculated neutron and matter density distributions of these two exotic nuclei. Besides, the noticeable difference that is found between the calculated overall proton and neutron rms radii also indicates a definite degree of halo structure. It is found that the structure of the halo neutrons for these two nuclei have

dominant $(1d)^2$ configurations. Also, it is found that the difference between the form factors of unstable exotic ${}^{12}\text{Be}$, ${}^{14}\text{Be}$ nuclei and those of the stable ${}^9\text{Be}$ nucleus is the difference in the center of mass correction which depends on the mass number and the size parameter b .

References:

1. Hansen P. G. and Jonson B. **1987**. The neutron halo of extremely neutron-rich nuclei. *Europhysics Letters*, **4**(4),pp:409-414.
2. Bowman J. D., Poskanzer A.M., R. G. and Butler G. W. ,**1973**. Discovery of two isotopes, ${}^{14}\text{Be}$ and ${}^{17}\text{B}$ at the limits of partial stability. *Physical Review Letter* **31**(9),pp:614-616.
3. Poskanzer A. M., Reeder P. L. and Dostrovsky I. **1965**. New delayed-neutron emitting isotope. *Physical Review* **138**,pp: 18-20.
4. Liatard E., Bruandet J. F., Glasser F.,Kox S., Tsan Ung Chan, Costa G. J., Heitz C., El Masri Y., Hanappe F., Bimbot R., Gullemaud-Mueller D.and Muller A. C. **1990**. Matter distribution in neutron-rich light nuclei and total reaction cross-section. *Europhysics Letters*, **13**(5),pp:401.
5. Tanihata I., Kobayashi T., Yamakawa O., Shimoura S., Ekuni K., Sugimoto K., Takahashi N.,Shimoda T. and Sato H. **1988**. Measurement of interaction cross sections using isotope beams of Be and B and isospin dependence of the Nuclear radii. *Physical. Letters B* ,**206**(4),pp:592-596.
6. Ozawa A., Kobayashi T., Sato H.,Hirata D., Tanihata I., Yamakawa O.,Omata K., Sugimoto K., Olson D., Christie W. and Wieman H.,**1994**. Interaction cross sections and radii of the mass number $A=17$ isobar (${}^{17}\text{N}$, ${}^{17}\text{F}$, and ${}^{17}\text{Ne}$). *Physical. Letters B* **334**(2),pp:18-22.
7. Talmi I. and Unna I. **1960**. Order of levels in the shell model and spin of ${}^{11}\text{Be}$. *Nuclear Physics* **19**,pp:225-242.
8. Kanada-Enyo Y. and Horiuchi H. **2003**. Cluster structures of the ground and excited states of ${}^{12}\text{Be}$ studied with antisymmetrized molecular dynamic.*Physical. Review C* **68**(1),pp: 014319-014336.
9. Kanada-Enyo Y. and Horiuchi H. **1995**. Structure of Li and Be isotopes studied with

- antisymmetrized molecular dynamic. *Physical. Review C* **52**(2): 628-646.
10. Neff T., Feldmeier H. and Roth R. **2005**. From the NN interaction to nuclear structure and reactions. *Nuclear Physics A* **752**,pp:321c-324c.
 11. Al- Khalili J. S., Tostevin J. A. and Thompson I.J. **1996**. Radii of halo nuclei from cross section measurements. *Physical. Review C.* **54**(4),pp: 1843-1852.
 12. Thompson I.J. and Zhukov M. V. **1996**. Structure and reactions of the $^{12,14}\text{Be}$ nuclei. *Physical. Review C.***53**(2),pp:708-714.
 13. Zahar M., Belbot M., Kolata J. J., Lamkin K., Thompson R., Orr N. A., Kelley J. H., Kryger R. A., Morrissey D. J., Sherrill B. M., Winger J. A., Winfield J. S. and Wuosmaa A. H. **1993**. Momentum distributions for $^{12,14}\text{Be}$ fragmentation. *Physical Review C* **48**(4),pp:R1484-R1487.
 14. Descouvemont P. **1995**. Halostructure of ^{14}Be in a microscopic $^{12}\text{Be} + n + n$ cluster model. *Physical. Review C.* **52**(2),pp: 704-410.
 15. Ilieva S., **2008**. Investigation of the nuclear matter density distributions of the exotic ^{12}Be , ^{14}Be and ^8B nuclei by elastic proton scattering in inverse kinematics. Ph.D. Thesis. am Fachbereich Physik, der Johannes Gutenberg-University, Mainz.
 16. De Forest T. Jr. and J.D.Walecka. **1966**. Electron scattering and Nuclear structure. *Adv. Physics* **15**, pp:1-109.
 17. Brown B. A, Radhi R. and Wildenthal B. H. **1983**. Electric quadrupole and hexadecupole nuclear excitation from the perspectives of electron scattering and modern shell model theory. *Physics Repots.* **101**(5),pp: 313-358.
 18. Radhi R. A. **1983**. Calculations of elastic and inelastic electron scattering in light nuclei with shell- model wave functions. Ph.D. Thesis. Department of Physics, Michigan State University, USA, p.11.
 19. Brown B. A., Etchegoyen A., Godwin N. S., Rae W. D. M., Richter W. A., Ormand W. E., Warburton E. K., Winfield J.S., Zhao L., and Zimmerman C. H. **2005**. Oxbash for windows PC.MSU-NSCL report number 1289.
 20. Glickman J. P., Bertozzi W., Buti T. N., Dixit S., Hersman F.W, HydeWright C. E., Hyns M. V, Lourie R. W.,Norum B. E., Kelly J. J, Berman B. L and Millener D. J. **1991**. Electron scattering from ^9Be . *Physical Review C* **43**(4),pp: 1740-1757.
 21. Audi G., Wapstra A. H and Thibault C. **2003**. The AME2003 Atomic Mass Evaluation (II). Tables, graphs and references, *Nuclear Physics A* **729**, pp:337-676.
 22. Chu Yan-Yun, Ren Zhong-Zhou, Wang Zai-Jun and Dong Tie- Kuang. **2010**. Charge densities of unstable nuclei with electron scattering. *Commun Theory Physics* **54**(2),pp: 347-354.
 23. Suzuki T., Kanungo R., Bochkarev O., Chulkov L., Cortine D., Fukuda M., Geissel H., Hellstrom M., Ivanov M., Janik R., Kimura K., Kobayaashi T., Korshennikov A. A., Munzenberg G., Nickel F., Ogloblin A. A., Ozawa A., Pfutzner M., Pribora V. and Simon H. **1999**. Nuclear radii of $^{17,19}\text{B}$ and ^{14}Be . *Nuclear Physics. A* **658**(4),pp:313- 326.
 24. Kuo T. T. S., Muether H. and Amir- Azimi-Nili K. **1996**. Realistic effective interactions for halo nuclei. *Nuclear Physics A.* **606**,pp:15-26.
 25. Kuo T. T. S., Krmpotic F. and Tzeng Y. **1997**. Suppression of core polarization in halo nuclei. *Physical Review Letters.* **78**(14),pp: 2708-2711.
 26. Krieger A., Blaum K., Bissell M. L., Frommgen N., Geppert CH., Hammen M., Kreim K., Kowalska M., Kraemer J., Neff T., Neugart R., Neyens G., Noertershauser W., Novotny CH., Sánchez R. and Yordanov D.T. **2012**. Nuclear Charge Radius of ^{12}Be . *Physical Review Letters.***108**(142501),pp: 1-5.
 27. Brown B. A. and Wildenthal B. H. ,**1988**. USD Hamiltonian for the sd shell. *Annual Review Nuclear and Particle Science.* **38**, pp:29-66.